

Preliminary Analysis of Single-Flash Geothermal Power Plant by Using Exergy Method: A Case Study from Ulubelu Geothermal Power Plant in Indonesia

Alimuddin*, Armansyah H. Tambunan**‡, Machfud***, Andi Novianto****

*Graduate School of Bogor Agricultural University, Indonesia

*Department of Geophysical Engineering, Lampung University, Indonesia

**Faculty of Agricultural Technology, Department of Mechanical and Bio-system Engineering, Bogor Agricultural University, Indonesia

***Faculty of Agricultural Technology, Department of Agroindustrial Technology, Bogor Agricultural University, Indonesia

****Coordinating Ministry of Economic Affairs, Indonesia

(alimuddin72@gmail.com, ahtambun@ipb.ac.id, machfud21@gmail.com, andinovianto@yahoo.com)

‡

Corresponding Author; Armansyah H. Tambunan, P.O. Box 220 Bogor 16002, ahtambun@ipb.ac.id

Received: 07.06.2018 Accepted:28.07.2018

Abstract- Indonesia is blessed with abundance of renewable energy sources, including geothermal, which needs to be used effectively to generate much required electric power in the country. Ulubelu Geothermal power plant is one of the newly installed facilities in Indonesia. Analysis on its performance is critical for further improvement of the generation efficiency. The main objective of this study is to analyze the performance of Ulubelu Geothermal power plant by using exergy analysis and to optimize the power output of the plant. The results showed that about 19.2% of the total mass flow steam from production wells was used to produce about 54,180 kW power, and around 80.8% of the mass flow is reinjected to the reservoir through the injection well. The rate of exergy input was 131,643 kW, out of which 83,364 kW was used for rotating the turbine. Exergy efficiency of the plant was 41.16%. Demister had the highest efficiency of 95.98%, while the highest exergy loss of 36.39% occurred at the separator. The optimization result indicated that the power output can be increased to 2600 kW if the steam pressure can be increased to 7.598 bar and the condenser pressure decreased to 0.06503 bar.

Keywords- Ulubelu; Geothermal power plant; Single-flash; Exergy analysis; Optimization; efficiency.

1. Introduction

Research on renewable energy topics are extremely relevant in the present time due to the rising energy demands and need of reducing greenhouse emissions [43] [44] [45]. Geothermal energy is one of the renewable energies that has high potency for replacing fossil fuel. Low carbon emissions and high sustainability make geothermal energy highly

attractive [1] [2]. Furthermore, geothermal has the potential to generate higher power of electricity compared to other renewable energy sources.

Indonesian government is currently implementing a 35,000 MW electricity generation program to achieve its electricity generation target. The policy target is to achieve 25% generation from renewable sources, including geothermal [3] [40]. Indonesia has high potency of geothermal

source since the country is located in the Pacific ring of fire which is volcanically active [4] [5] [6]. Geothermal potency in Indonesia is 29 GW, but only 1.5 GW of which has been utilized in 2015 [7] [5].

Geothermal power plants use steam from the production well to generate electricity. The technical specification of geothermal plants depend on the nature of the steam produced from the well. If the type of geothermal system reservoir is vapor-dominated, it may be routed directly to the turbines in order to generate electricity. However, If the system is liquid-dominated, it requires a separation process before it is flow to the turbine and generate the electricity [8] [9]. Geothermal power plants can be widely classified into dry, single-flash, double-flash, triple-flash, binary, flash-binary and hybrid types [10]. Flash type power plants are calssified base on the fluid and reservoir types. Single flash type is the most commonly installed plant around the world, 185 out of a total of 573 geothermal plants, and it is responsible for generating 5146 MW of electricity worldwide [11] [10] [12].

Performance analysis of geothermal power plant is critical in order to improve the system, both in terms of process and equipment. One of the effective tools for such analysis is exergy analysis, studied extensively over the last few decades [13] [14] [15] [41] and has been used for analyzing geothermal power plant [16][42]. The exergy analysis is aimed at measuring the performance of the plant for increasing the efficiency of energy resources utilization and for quantifying the location, type, and the magnitude of waste and loss [9] [17] [18] [19].

The performance of a geothermal power plant is determined by its efficiency in converting the energy stored in the steam to electric energy. The objectives of this study are (1) to analyze the performance of the geothermal power plant in terms of components and overall efficiency of the system by employing exergy analysis, and (2) to optimize the power output of the plant.

2. Description of Ulubelu Geothermal Power Plant

Ulubelu geothermal power plant is located in Muara Dua Sub-District, Tanggamus District, Lampung Province of Indonesia, at an altitude of 500 to 1500 meters above the sea level. Annual average ambient temperature of the location is 22.8°C and atmospheric pressure is 0.921 bar [20]. Two units of the power plant have been operating since 2012 [21]. A third unit using steam from eleven production wells in four clusters, has recently started operation, while a fourth unit is under construction [21].

The wells produce moist steam with an average temperature of 265°C and an average enthalpy of 1160 kJ/kg [22] [20] [23]. The power plant used at Ulubelu is of single-flash type, each unit capable of producing 55 MW of electrical power [24].

The production wells are located at 770 to 853 meters altitude above the sea level, and are distributed under three clusters. Clusters B and C consist of four wells each, while cluster D consists of three wells. The depth of the production wells range from 1553 to 2537 meters [20]. The injection wells are located at an altitude of 688 to 702 meters above the sea level. They are distributed into two clusters, A and F, each

consisting of three injection wells. The depth of the injection wells range from 1650 to 1793 meters.

3. Method of Analysis

3.1 Energy and exergy analysis

The flow of energy and exergy in the power plant system was analyzed following the schematic diagram shown in Figure 1. Numbered node was labeled to the inlet and outlet of each of the unit process, as well as to any separating branch, where the property of the steam to be evaluated. The property at each node was then used to determine its energy and exergy by equations (1), (2), and (3) [25] [26]:

$$\dot{E}_i = \dot{m}_i h_i \quad (1)$$

$$e_i = h_i - h_o - T_o(s_i - s_o) \quad (2)$$

$$\dot{X}_i = \dot{m}_i e_i \quad (3)$$

where, \dot{E}_i is the energy flow rate (kW), e is specific exergy (kJ/kg), \dot{X}_i is exergy flow rate (kW), \dot{m}_i is steam mass flow rate (kg/s), h is specific enthalpy (kJ/kg), s is specific entropy (kJ/kg-K) and T is temperature (°C). Subscript i denotes the node i , and subscript o denotes the dead state (reference state). Turbine power \dot{W}_{tur} (kW) and electrical power \dot{W}_{net} (kW) were calculated using equation (4) and (5), respectively:

$$\dot{W}_{tur} = \dot{m}_4 \cdot (h_4 - h_5) \quad (4)$$

$$\dot{W}_{net} = \dot{W}_{tur} \cdot \eta_{gen} \quad (5)$$

where, h_4 is steam enthalpy entering the turbine, h_5 is enthalpy of steam out of the turbine, and η_{gen} is generator efficiency. Energy and exergy balance equations at each unit process can be expressed as in equation (6) and (7) respectively. Here, \dot{I} is the rate of irreversibility (kW). The exergy is considered as exergy transferred if it is transferred to the next unit process heading to electric generator end, while considered as exergy waste if it is transferred to other pathways such as to rejection well or basin.

$$\sum_{inlet} \dot{E} = \sum_{outlet} \dot{E} + \sum_{loss} \dot{E} \quad (6)$$

$$\sum_{inlet} \dot{X} = \sum_{trans} \dot{X} + \sum_{waste} \dot{E} + \dot{I} \quad (7)$$

The energy efficiency is defined as the ratio of total energy rate at the outlet to the total energy rate at the inlet of each unit process, as depicted in equation (8). The exergy efficiency, or second law efficiency of the single-flash geothermal power plant, is defined as the ratio of total rate of exergy transferred to the total rate of exergy at the inlet of the unit process, as shown in equation (9) [26] [18]. Net efficiency of the power plant is then calculated as the ratio of power produced by the electric generator to the total exergy rate at node 1, as depicted in equation (10).

$$\eta_I = \frac{\sum \dot{E}_{out}}{\sum \dot{E}_{in}} \quad (8)$$

$$\eta_{II} = \frac{\sum \dot{X}_{transfer}}{\sum \dot{X}_{in}} \quad (9)$$

$$\eta_{net} = \frac{\sum \dot{W}_{net}}{\sum \dot{X}_1} \quad (10)$$

where, η_I is the energy efficiency (%), η_{II} is exergy efficiency (%), and η_{net} is the efficiency of the power plant.

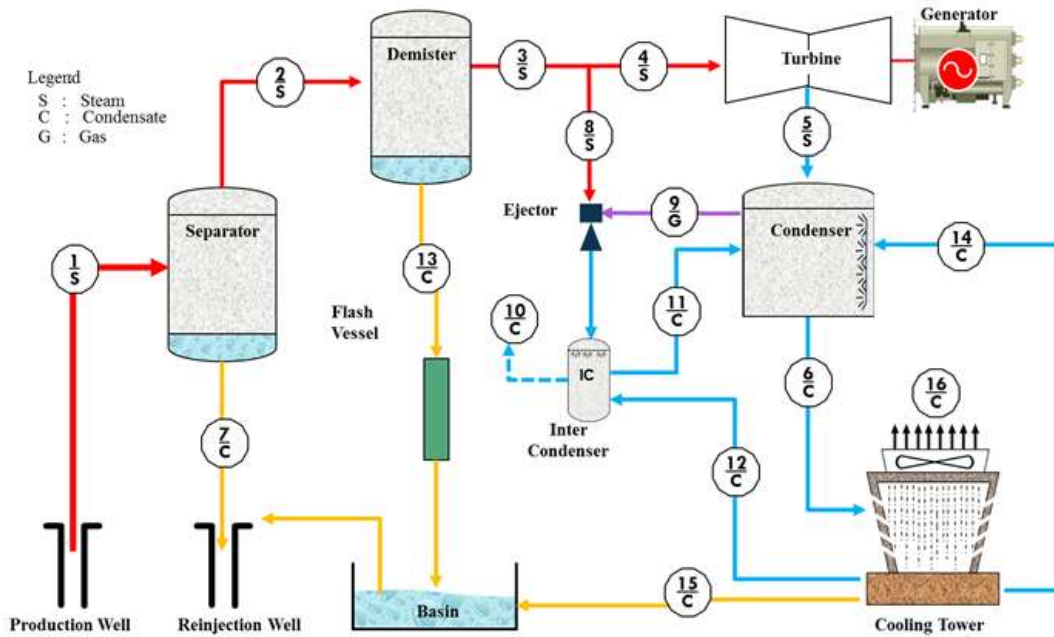


Fig. 1. Simplified schematic diagram of Ulubelu Geothermal Power Plant and positioning of states along the process line

4. Source of Data

The data required for this study was obtained from Ulubelu geothermal power plant, recorded as pressure, temperature, and mass flow rate of the steam at each node. Other properties of the steam were evaluated by using Engineering Equation Solver (EES), where the average pressure and temperature were utilized as independent properties. Other data required for the analysis, but unavailable at or unrecorded by the Ulubelu geothermal power plant were evaluated from appropriate heat and mass balance of the system or unit process. All calculations were conducted by using the Engineering Equation Software (EES).

5. Results and Discussion

5.1. The performance of the Ulubelu Geothermal Power Plant

The overall characteristics of the data used in this study are illustrated in Figure 2. The steam produced from reservoirs through the production wells are of dual phase type and need to be separated into steam-vapor and brine. Brine is re-injected into the reservoir through the injection wells and steam-vapor is sent to the turbine to produce the electrical energy.

The steam flow starts from the production well and then it is channeled into separator (1) with average steam temperature of 170.3°C, a pressure of 7.84 bar, and a mass flow rate of 522.0 kg/s. Such conditions separate the liquid and dry steam, as presented in Figure 2 and Figure 5. The liquid steam (brine) then goes to the injection well (7) with mass flow rate of 415.0 kg/s and steam-vapor passes on to the demister (2) with an average steam temperature of 170.3°C, a

pressure of 7.84 bar, and a mass flow rate of 106.3 kg/s. Following this, the steam flows to the turbine with a mass flow rate of 100.3 kg/s, a pressure of 7.39 bar, and a temperature of 167.6°C, as presented in Figure 3 and Figure 5 respectively. Energy content of the steam is converted into mechanical energy in the turbine, and then into electrical energy through a generator, which produces electrical power of around 54.3 MW. The fluid from the turbine passes to the condenser which transforms steam fluid into liquid with an average temperature 42.6°C and a pressure of 0.083 bar, as presented in Figure 4a and 4b respectively. The liquid from the condenser then passes on to the cooling tower to where the temperature is brought down to 26.4°C which is then re-injected into the reservoir. Uncondensed fluid gasses are released in the environment.

The plant performance was analyzed from the relation of the steam parameters, such as pressure, temperature, mass flow and power output of the plant. The analysis was based on the plant steam flow data from the separator and the turbine components. The relation of steam parameters passing through separator and turbine, and the power output of plant are presented in Figure 3a and 3b respectively.

Based on the plant operational data, Figure 5 reveals a mass flow rate of 522.0 kg/s while entering into the separator. Approximately 19.2% or 100.3 kg/s of the mass flow continues to the turbine and around 80.7% or 421.7 kg/s of the mass flow is re-injected to the reservoir through the injection well. The mass flow entering into the turbine produces an average output of ~54.3 MW electrical power.

Therefore, from the above information, it is deduced that the Ulubelu geothermal power plant with a steam mass flow rate of 1 kg/s will produce the average power output of approximately 0.55 MW. According to other studies conducted on Dieng geothermal power plant, the average power output was found to be 0.53 MW for 1 kg/s of the steam

mass flow rate with the higher percentage of the turbine steam utilization, viz. 29.4% [27]. The steam pressure and the temperature decreases around 0.36 bar and 2.2°C respectively. The reduction in steam pressure is calculated based on the difference of the average steam pressure at the separator and

at the turbine. Similarly, the lowering of temperature can also be calculated.

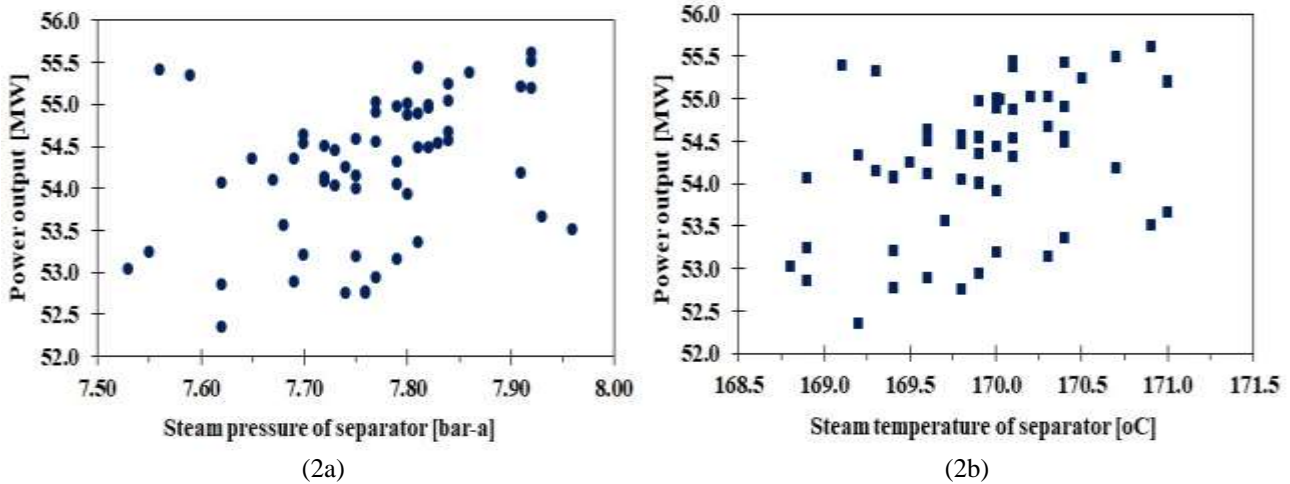


Fig. 2. Relationship between the property of steam at the separator inlet and the actual power output of the power plant (a) Steam pressure, (b) Steam temperature

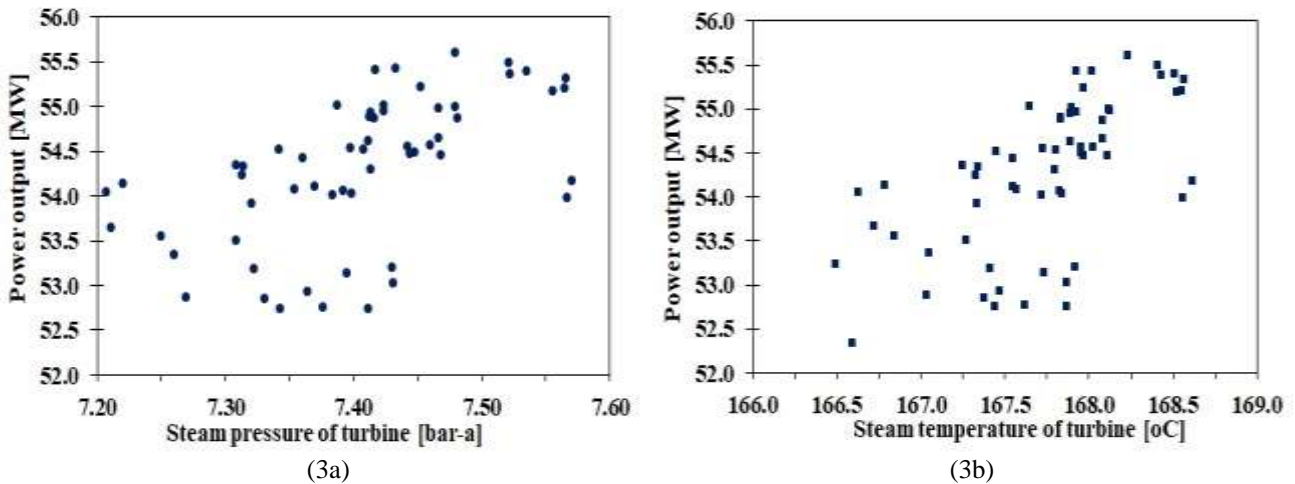
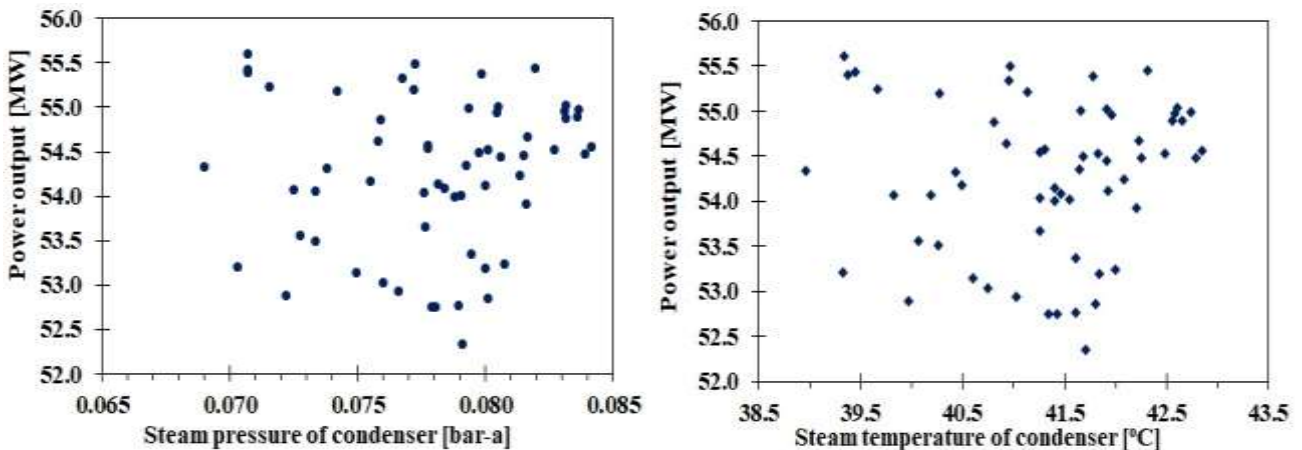
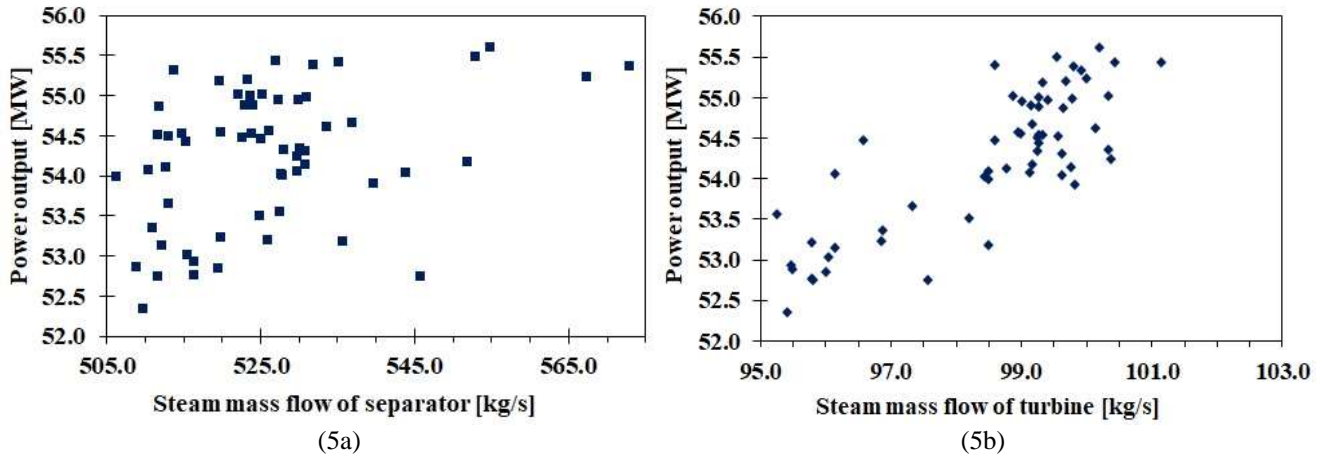


Fig. 3. Relationship between the property of steam at the turbine inlet and the actual power output of the power plant (a) Steam pressure, (b) Steam temperature



(4a) (4b)
Fig. 4. Relationship between the property of steam at the condenser inlet and the actual power output of the power plant (a) Steam pressure, (b) Steam temperature



(5a) (5b)
Fig. 5 Relationship between the steam mass flow at the separator inlet and the turbine inlet with the actual power output of the power plant (a) Separator inlet, (b) Turbine inlet

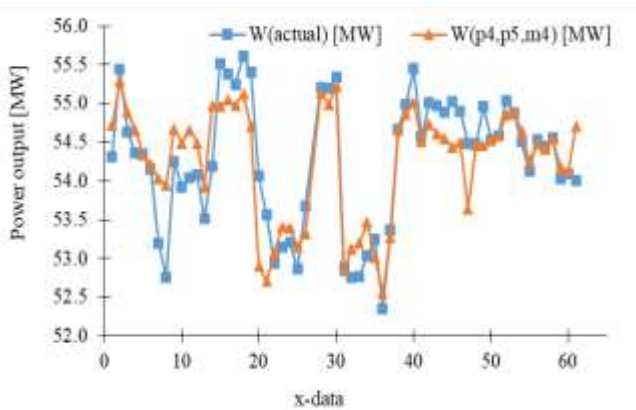


Fig. 6. Relationship between the property of steam at the turbine inlet and of condenser and the actual power output

Figure 6 describes the relation between pressure (p_4) and the steam mass flow (\dot{m}_4) at the turbine and pressure at the condenser (p_5) based on the recorded data of the operating power plant. This relation is represented in the following equation:

$$\dot{W}(p_4, p_5, \dot{m}_4) = -1.0108 + 2.7234 * p_4 - 5.7570 * p_5 + 0.3610 * \dot{m}_4 \quad (11)$$

Equation (11) indicates that maximizing pressure and mass flow at a turbine and minimizing pressure at a condenser, can in turn maximize the power output of the power plant.

5.2. The energy and exergy analysis of geothermal steam flow

This research uses the actual data and other supporting data for analyzing energy and exergy in the power plant. Thermodynamic property, energy, and exergy of the steam at each state in the process line as calculated from real operational data at the power plant are shown in Table 1. The thermodynamic analysis of the steam flow was based on the cycle as shown in Figure 1. The table presents pressure (p), temperature (T), and mass flow rate (\dot{m}) based on the plant operational data. The enthalpy (h) and entropy (s) refer to the properties of the saturated water table [25]. The energy flow rate (\dot{E}) is calculated by Equation (1), specific exergy (e) is calculated by Equation (2), and exergy flow rate (\dot{X}) is calculated by Equation (3). The environmental reference to calculate the specific exergy is temperature (T_o) of 25°C and pressure (p_o) of 1 bar. All calculations were performed using EES software.

The geothermal power plant system follows the thermodynamics law in the context of energy conservation and geo-fluid mass conservation according to given parameters [28]. The state of the geothermal fluid in the cycle of a geothermal power plant is described by temperature-entropy (T-s) and pressure-enthalpy (p-h) diagram as shown in Figure 7 by using EES software. The Figure 7 is obtained from the values of temperature, pressure, enthalpy, and entropy data as presented in Table 1

Table 1. Thermodynamic property, energy, and exergy of the steam at each state in the process line.

State [i]	\dot{m} [kg/s]	T [° C]	p [bar]	h [kJ/kg]	s [kJ/kg-K]	e [kJ/kg]	\dot{E} [kW]	\dot{X} [kW]
1	522.0	170.3	7.84	1138	2.986	252.2	593,870	131,643
2	106.3	170.3	7.84	2768	6.669	784.2	294,245	83,364

3	103.1	167.6	7.39	2766	6.690	775.8	285,162	79,991
4	100.3	167.6	7.39	2766	6.690	775.8	277,390	77,811
5	100.3	42.6	0.083	2197	7.008	112.3	220,359	11,264
6	3351	41.4	0.083	173.4	0.591	1.825	580,931	6116
7	415.7	170.3	7.84	720.6	2.045	115.5	299,552	48,025
8	2.81	167.6	7.39	2766	6.690	775.8	7771	2180
9	3.20	34.0	-	2179	7.122	60.24	6973	192.8
10	2.39	36.1	-	151.2	0.520	0.846	361.3	2.023
11	218.8	36.1	-	151.2	0.520	0.846	33,091	185.2
12	215.2	28.0	-	117.3	0.409	0.063	25,250	13.63
13	3.19	167.6	7.39	708.8	2.018	111.6	2261	356.1
14	3035	28.0	-	117.3	0.409	0.063	356,023	192.2
15	21.28	28.0	-	117.3	0.409	0.063	2496	1.35
16	79.44	40.7	-	170.4	0.582	1.675	13,539	133.1

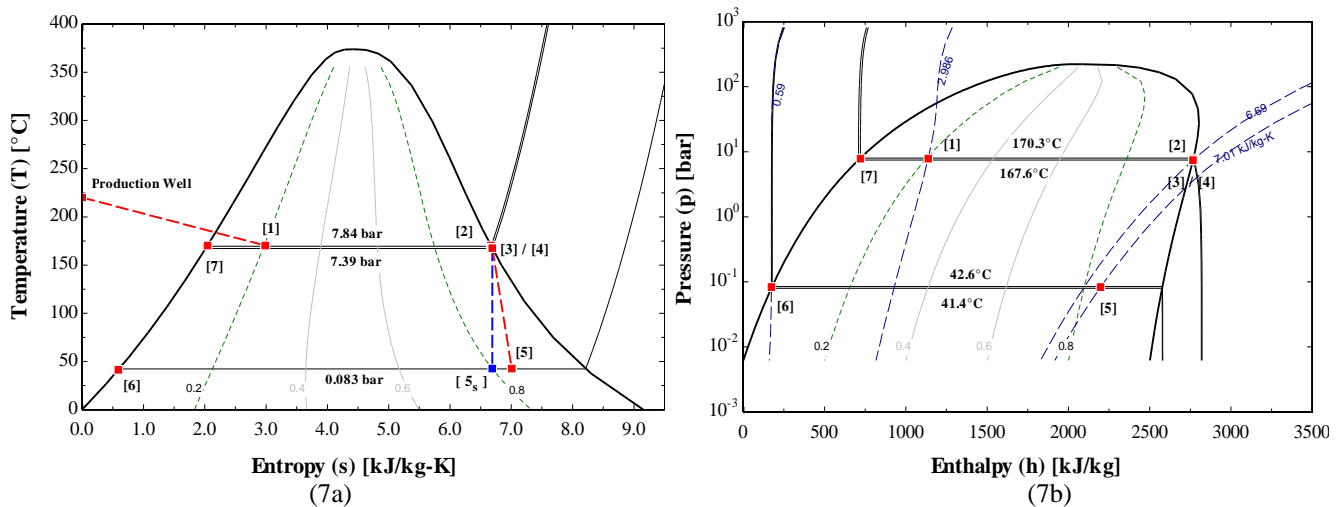


Fig. 7. The geothermal fluid in the cycle of a geothermal power plant is described by (a) temperature-entropy (T-s) graph and (b) pressure-enthalpy (p-h) graph

Figure 7(a) shows the relation between entropy and temperature of the steam, while Figure 7(b) shows the relation between enthalpy and pressure of the steam. Geothermal steam experienced an entropy increase of 0.318 kJ/Kg-K and an enthalpy decrease of 569 kJ/kg after being used to rotate the turbine, with a reduction of 125°C temperature and 7.31 bar pressure. This is achieved in the condenser when the steam is sprayed with cool water (28°C) from the cooling tower, i.e. step-4 and step-5.

The initial state of the steam is excluded from the saturated state with a temperature around 260°C [22] and then flows to a separator with quality 0.2 [21] at temperature 170.3°C and pressure 7.84 bar. The steam produced from reservoir through a production well originally exists as single phase steam where water is compressed in the reservoir. It is assumed that the steam flow from a reservoir to wellhead through the well hole is isenthalpic in nature. During this process, the steam from a production well flows into the separator. After that, the steam continues to a demister and then to the turbine and further to the condenser and cooling tower. Steam-vapour with quality 0.84 enters into the turbine at a temperature of 167.6°C, a pressure of 7.39 bar and an

entropy of 6.90 kJ/kg-K. This result is in agreement with previous findings [9] [29] [30] [31].

The exergy flow consists of exergy transfer, exergy brine/waste, destruction of exergy, and power output at the plant as shown in Grassmann diagram in Figure 8. The total exergy flow rate entering into the plant is 131,643 kW. A total of 83,364 kW of exergy transfer from separator is flown to a demister, then 77,811 kW is passed to the turbine to rotate the blades. A potential exergy in form of brine is not utilized and as large as 48,025 kW worth power is injected back in the well. The destruction of exergy is caused by the irreversibility in the plant system which occurs at each component of the plant. A total destruction of exergy is around 28,944 kW or 21.99% and waste of exergy is around 494 kW or 0.37% of the total exergy entering into the plant.

The exergy from the well before the separator is 131,643 kW. The unutilized exergy rate at state 7 is 48,025 kW in the form of steam-liquid which gets separated from the separator. The steam from step 7 is re-injected to the reservoir through reinjection well. The exergy flow rate at state 4 is in steam-vapor ~77,811 kW. The result of calculating the turbine power by using equation (4) is approximately 57,031 kW and the

generator power by using equation (5) produces approximately 54,180 kW with the generator efficiency of 95%.

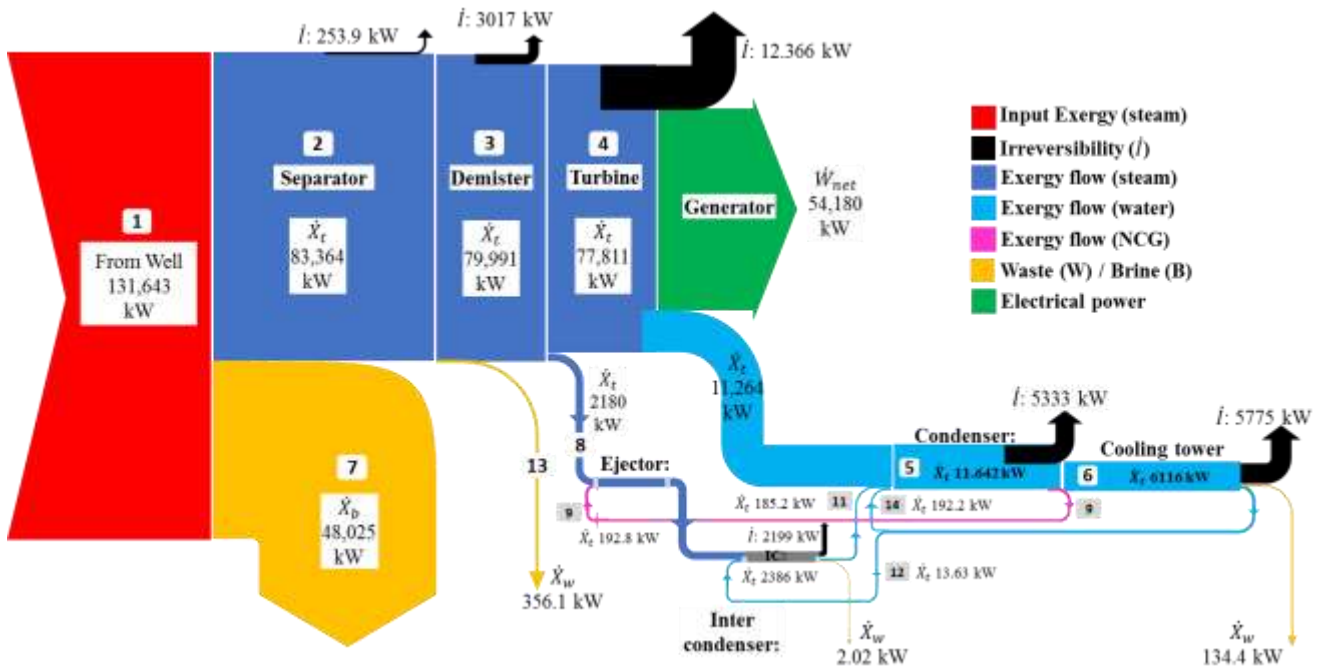


Fig. 8. Grassmann diagram of the overall exergy flow at the plant cycle

5.3. The energy and exergy efficiency of geothermal power plant

The energy and exergy efficiency of the plant can be calculated by Equation (9) and (10), and the results have been presented in Table 2 and 3. The calculation was conducted in each main component of the plant, such as the separator, demister, turbine-generator, condenser, inter-condenser, cooling tower, and the overall power plant.

The most energy efficient is the demister utilizing 96.91% energy and the least energy efficient is the turbine-generator utilizing only 19.59% energy. This is due to very little energy loss, i.e. 2852 kW at the demister. The turbine converts mechanical energy into electrical energy as large as 54,180 kW. The energy efficiency of the separator is also low (49.55%), and the energy loss is large (299,625 kW) in the form of brine that is not utilized.

The first row in Table 3 is the separator which has exergy input rate of approximately 131,643 kW worth of steam from the production well in form of mixed liquid-vapor. The exergy was calculated based on mass flow rate, enthalpy, and entropy. The steam state is assumed to be in the liquid saturated state. The exergy output rate from the separator component consists

of steam-vapor exergy rate which flows to the demister and then to the turbine. The steam-liquid exergy rate or brine is reinjected to the reservoir through the reinjection well. The efficiency according to the second law thermodynamics at this separator is 63.33% with fluid enthalpy of 1138 kJ/kg at an ambient temperature of 26°C. Studies on separator efficiency in Dieng geothermal power plant calculated a value of 86.50% with fluid enthalpy of 1401 kJ/kg and at an ambient temperature of 18°C [27]. In Olkaria geothermal power plant, an efficiency of 68% was calculated with fluid enthalpy of 2000 kJ/kg and an ambient temperature of 20°C [32].

The highest exergy efficiency of 95.95% is obtained at the demister. This is because the steam flow at that component does not result into loss of mass flow. Studies in Kamojang geothermal power plant produced an efficiency of 99.66% [33] and the research in Dieng geothermal power plant produced around 99.63% efficiency [27]. The highest irreversible exergy of 12,366 kW is obtained at the turbine-generator component. The irreversibility rates in the steam generator is associated with waste and heat transfer exergy [34]. This may occur due to the expansion across the blades [35].

Table 2. The energy rate calculation result at each plant component

Components	\dot{E}_{inlet} [kW]	\dot{E}_{outlet} [kW]	\dot{E}_{loss} [kW]	η_I [%]
Separator	593,870	294,245	299,625	49.55
Demister	294,245	285,162	9083	96.91

Turbine-generator	277,390	274,539	2852	19.59
Condenser	609,463	587,893	21,570	96.46
Inter-condenser	39,987	33,082	6905	82.73
Cooling tower	580,920	381,265	199,655	65.63

Table 3. The exergy rate calculation result at the plant components

Components	\dot{X}_{in} [kW]	\dot{X}_t [kW]	\dot{X}_b [kW]	\dot{X}_w [kW]	\dot{W}_{net} [kW]	$\dot{I}_{irr.}$ [kW]	η_{II} [%]
Separator	131,643	83,364	48,025	-	-	253.9	63.33
Demister	83,364	79,991	-	356.1	-	3017	95.95
Turbine-generator	77,811	11,264	-	-	54,180	12,366	69.63
Condenser	11,642	6308	-	-	-	5334	52.53
Inter-condenser	2386	185.2	-	2.02	-	2199	7.76
Cooling tower	6116	205.9	-	134.4	-	5776	3.39

The overall exergy efficiency of Ulubelu geothermal power plant is calculated to be 41.16% with power output of approximately 54,180 kW. This result is higher compared to other studies. Jalilinasrabad et al. [36] calculated the exergy efficiency of 32.73% with power output of 31.1 MW, Unverdi and Cerci [37] calculated an exergy efficiency of 35.34%, and Pambudi et al. [27] calculated an exergy efficiency of 36.48% with power output of 21.71 MW.

5.4. The exergy losses of geothermal power plant

Grassmann diagram in Figure 8 shows the percent value of exergy loss at each component in the power plant. Total exergy loss is describe by the exergy flow rate which enters into the plant, the exergy rate which is lost from each plant component, and the utilized exergy rate for producing the plant power output. Total exergy flow rate which enters into the plant is 131,643 kW, meanwhile, the utilized exergy flow rate for producing the plant output power is around 54,180 kW (41.16%).

Figure 9 reveals that the brine at the separator component causes the highest loss in exergy of 48,025 kW (36.48 %), followed by demister and turbine with exergy loss rate of 3017 kW (2.29 %) and 12,366 kW (9.39%) respectively. The condenser and inter-condenser components also cause loss in the exergy of 5333 kW (4.05%) and 2199 kW (1.67%), respectively. The cooling tower component loses 5775 kW (4.39 %) of the exergy and the condensate from the demister-inter condenser-cooling tower causes 492.52 kW (0.37%) exergy loss. The two-phase steam resulted in higher exergy loss rate at a separator component than others because brine, as a result of separating process, is not utilized. In other studies, Cerci [38] calculated the exergy loss at the brine to be 46.9% and Pambudi et al. [27] calculated a 17.19%. exergy loss Jalilinasrabad et al. [36] concluded that the highest exergy destruction takes place at the condenser, the turbine, and the disposed waste brine with 23.35%, 4.91%, 41.44%, respectively of total exergy destruction in the plant.

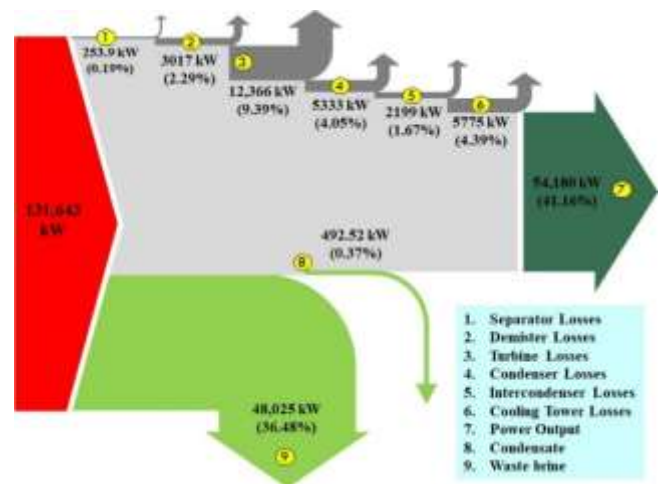


Fig. 9. Grassmann diagram of the loss of exergy in the plants

5.5. Optimization of the geothermal powerplant

The Ulubelu geothermal powerplant has a power output of approximately 54,180 kW with pressure at the turbine and the condenser at 7.39 and 0.083 bar, respectively. The steam mass flow rate at the turbine is 100.3 kg/s. The plant efficiency can reach to about 41.16%. Based on the analysis of parameters using equation (11), the steam pressure at the turbine and condenser is an important parameter influencing power output, besides steam mass flow. The relation between the power output and the pressure was calculated by simulating the pressure at the turbine and the condenser. The optimization process was performed by EES software using the maximum and minimum calculation tool through the genetic method [39].

Parametric simulation was performed at different condenser pressures of 0.065, 0.07, 0.08, and 0.09 bar. The result of simulation showed that output power maximum can be achieved at 0.065 bar of condenser pressure. Meanwhile the minimum of output power can be achieved at 0.09 bar of

condenser pressure and minimum turbine pressure (Figure 10).

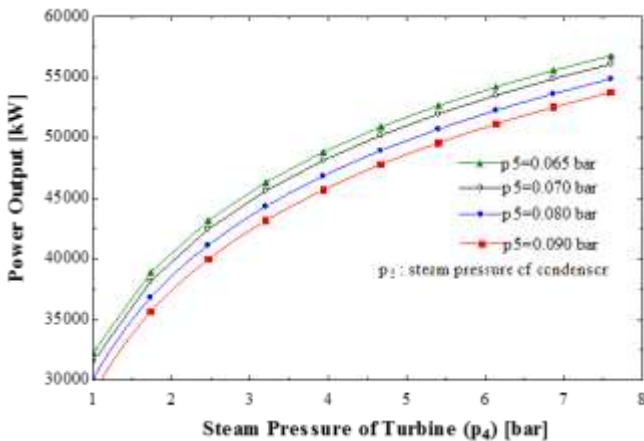


Fig. 10. The simulation result of calculating the varied steam pressure at the condenser

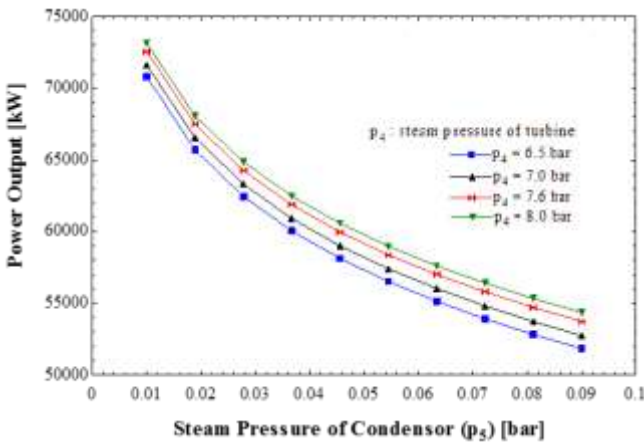


Fig. 11. The simulation result of calculating the varied steam pressure at the turbine

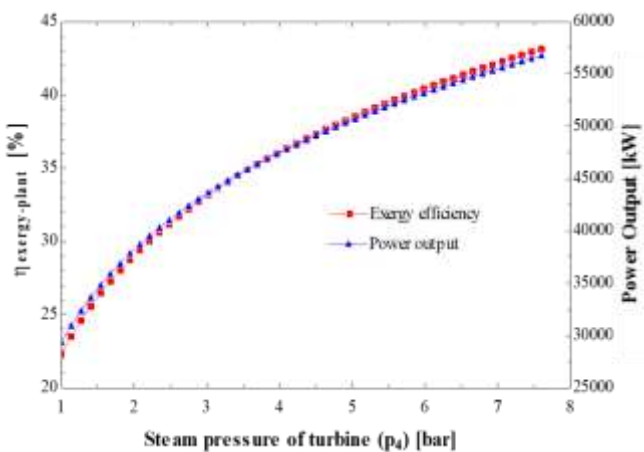


Fig. 12. The relationship of steam pressure at the turbine, exergy efficiency, and power output of the plant

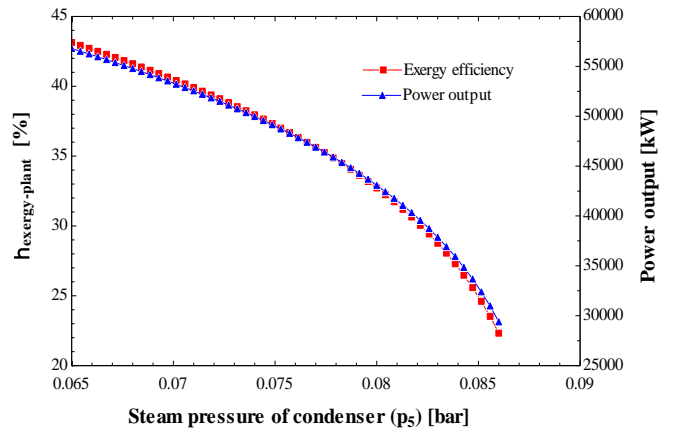


Fig. 13. The relationship of steam pressure at the condenser, exergy efficiency, and power output of the plant

Moreover, parametric simulation was done at different values of turbine pressure at 6.5, 7.0, 7.6 and 8.0 bar. The simulation results showed that maximum output power occurred at 8.0 bar turbine pressure and minimum condenser pressure. In contrast, the minimum of output power occurred at 6.5 bar turbine pressure and maximum steam condenser pressure (Figure 11). Therefore, increasing the steam pressure at the turbine will increase the exergy efficiency and power output of the plant (Figure 12) and increasing the steam pressure at the condenser will decrease the exergy efficiency and power output of the plant (Figure 13).

Based on the parametric simulation, the optimization process was done with min/max tool in EES software with two independent variables i.e. turbine pressure and condenser pressure, while the dependent variable is power output. The boundary value for turbine steam pressure was 6.5 to 7.6 bar. Meanwhile the limit of steam condenser pressure was 0.065 to 0.1 bar. These values were adapted from the manuals of turbine and condenser components.

The optimization result of the power plant produced the power output of approximately 56,778 kW with the steam pressure to the turbine at about 7.598 bar and the condenser pressure of about 0.06503 bar, as well as the steam mass flow at 100.3 kg/s. Under such conditions, the exergy efficiency reached 43.14% with an increased power output of 2.60 MW. When turbine pressure was increased by 0.21 bar and the condenser pressure was reduced by 0.018 bar, the plant efficiency increased by 1.98%. This result differs from other studies. The study in Dieng geothermal power plant revealed that power output could be increased by 20 kW on decreasing the separator pressure from 10 bar to 9 bar [27]. Meanwhile, Jalilinasrabady et al. [36] calculated the optimum separation pressure value of 5.5 bar. The exhaust steam quality from the turbine in our study was around 0.835, as shown in Figure 14 and this value is lower than the assumption of 0.86 by Jalilinasrabady et al. [36].

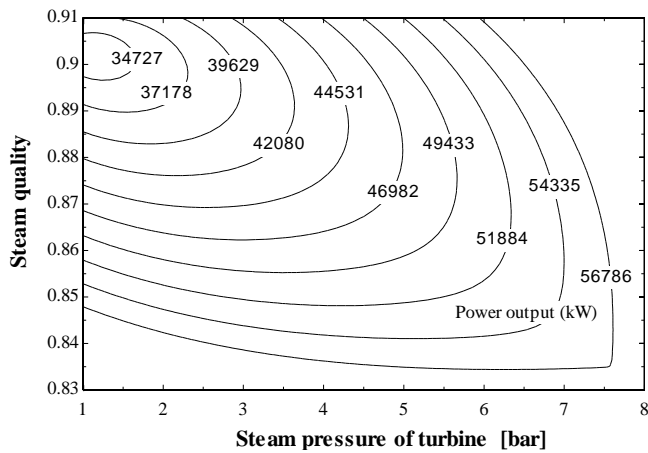


Fig. 14. Exhaust steam quality from the turbine

6. Conclusion

The exergy analysis showed that the exergy input in the plant is approximately 131,643 kW out of which, 83,364 kW is utilized to rotate the turbine, while the rate of unutilized exergy is 48,276 kW. The overall exergy efficiency of Ulubelu geothermal power plant is calculated to be 41.16% with power output of approximately 54,180 kW. The highest exergy efficiency is 95.98% in the demister component and the lowest exergy efficiency is 3.39% in the cooling tower component. The highest exergy loss at separator component is about 36.39% of the available total exergy, and the utilized exergy rate is only around 41.31% used to produce the electrical power.

The optimization result indicates that the power output can be increased by 2.6 MW if the steam pressure at the turbine is increased from 7.39 bar to 7.60 bar and the steam pressure at the condenser is decreased from 0.084 bar to 0.065 bar with an assumption that the mass flow rate is 100.3 kg/s.

Acknowledgements

We will like to convey our thanks to Ministry of Research, Technology, and Higher Education for financially supporting our research, PT PLN and Ulubelu geothermal power plant for allowing us to conduct the research and providing access to the data needed for the work..

References:

[1] H. Ármannsson, T. Fridriksson, and B. R. Kristjánsson, "CO₂ emissions from geothermal power plants and natural geothermal activity in Iceland," *Geothermics*, vol. 34, no. 3, pp. 286–296, 2005.

[2] M. Aneke, B. Agnew, and C. Underwood, "Performance analysis of the Chena binary geothermal power plant," *Applied Thermal Engineering*, vol. 31, no. 10, pp. 1825–1832, 2011.

[3] [BPPT] Badan Pengkajian dan Penerapan Teknologi, *Outlook Energi Indonesia 2016: pengembangan energi untuk mendukung industri hijau*. Jakarta (ID): Badan Pengkajian dan Penerapan Teknologi: Pusat Teknologi Sumberdaya Energi dan Industri Kimia BPPT, 2016.

[4] J. Stimac, G. Nordquist, A. Suminar, and L. Sirad-Azwar, "An overview of the Awibengkok geothermal system, Indonesia," *Geothermics*, vol. 37, no. 3, pp. 300–331, 2008.

[5] N. A. Pambudi, "Geothermal power generation in Indonesia, a country within the ring of fire: Current status, future development and policy," *Renewable and Sustainable Energy Reviews*, vol. 81, no. 2, pp. 2893–2901, 2018.

[6] U. Sumotarto, "Geothermal Energy Potential of Arjuno and Welirang Volcanoes Area , East Java , Indonesia," *International Journal of Renewable Energy Research*, vol. 8, no. 1, 2018.

[7] A. Poernomo, S. Satar, P. Effendi, A. Kusuma, T. Azimudin, and S. Sudarwo, "An Overview of Indonesia Geothermal Development – Current Status and Its Challenges," in *Proceedings World Geothermal Congress, 19-25 April 2015*, 2015, no. 19–25 April 2015, pp. 19–25.

[8] M. P. Hochstein and S. Sudarman, "History of geothermal exploration in Indonesia from 1970 to 2000," *Geothermics*, vol. 37, no. 3, pp. 220–266, 2008.

[9] R. DiPippo, "Geothermal double-flash plant with interstage reheating: An updated and expanded thermal and exergetic analysis and optimization," *Geothermics*, vol. 48, pp. 121–131, 2013.

[10] R. DiPippo, *Geothermal Power Plants: Principles , Applications , Case Studies and Environmental Impact Third Edition*, 3rd ed. Oxford (UK): Butterworth-Heinemann, Elsevier, 2016.

[11] A. Dagdas, "Performance optimisation of the combined single flash binary geothermal power plant," *International Journal of Exergy*, vol. 8, no. 2, p. 194, 2011.

[12] R. Venegas, S. Kuravi, K. Kota, and M. H. McCay, "Comparative Analysis of Designing Solar and Geothermal Power Plants : A Case Study," *International Journal of Renewable Energy Research*, vol. 8, no. 1, 2018.

[13] A. H. Tambunan, Furqon, Joelianingsih, T. Araki, and H. Nabetani, "Energy and Exergy Analysis on Heat Recirculation in Non-Catalytic Reaction of," *Teknologi Energi*, vol. 1, no. 13, pp. 11–22, 2011.

[14] H. Ganjehsarabi, A. Gungor, and I. Dincer, "Exergoeconomic evaluation of a geothermal power plant," *International Journal of Exergy*, vol. 14, no. 3, pp. 303–319, 2014.

[15] A. Vadiée and M. Yaghoubi, "Exergy Analysis of the Solar Blind System integrated with a Commercial Solar Greenhouse," *International Journal of Renewable Energy Research*, vol. 6, no. 3, 2016.

[16] G. Gokcen and N. Yildirim, "Effect of Non-Condensable Gases on geothermal power plant performance. Case study: Kizildere Geothermal Power Plant-Turkey," *International Journal of Exergy*, vol. 5,

- no. 5/6, pp. 684–695, 2008.
- [17] M. Gorji-Bandpy and V. Ebrahimian, “Exergy analysis of a steam power plant: A case study in Iran,” *International Journal of Exergy*, vol. 4, no. 1, pp. 54–73, 2007.
- [18] M. Kanoglu, Y. A. Cengel, and I. Dincer, *Efficiency Evaluation of Energy Systems*. New York (US): SpringerBriefs in Energy, 2012.
- [19] R. DiPippo, “Geothermal power plants: Evolution and performance assessments,” *Geothermics*, vol. 53, pp. 291–307, 2015.
- [20] A. N. Purwono, “Comparison and Selection of a Steam Gathering System in Ulubelu Geothermal Project , Sumatera , Indonesia,” *UNU Geothermal Training Programme*, vol. Reports 26, pp. 525–562, 2010.
- [21] D. M. Yuniar, P. Hastuti, and M. Silaban, “Ulubelu , First Year Reservoir Monitoring,” in *Proceedings World Geothermal Congress, 19-25 April 2015*, 2015, no. 19–25 April 2015, pp. 2–6.
- [22] Y. Daud, S. Sudarman, and K. Ushijima, “Integrated Geophysical Studies of the Ulubelu Geothermal Field , South Sumatera , Indonesia,” in *Proceedings World Geothermal Congress, May 28 - June 10, 2000*, 2000, no. May 28-June 10, 2000, pp. 1071–1076.
- [23] Mulyanto, A. Puspadianti, J. P. Giriarmo, and D. B. Hartanto, “The Initial-State Geochemistry as a Baseline for Geochemical Monitoring at Ulubelu Geothermal Field , Indonesia,” in *Proceedings World Geothermal Congress, 19-25 April 2015*, 2015, no. 19–25 April 2015, pp. 2–6.
- [24] M. Agani, S. Patangke, D. B. Hartanto, and M. Silaban, “Opportunity and Barriers to Develop a Bottoming Unit by Utilizing Separated Hot Brine in Ulubelu, Indonesia,” in *Proceedings World Geothermal Congress, 19-25 April 2015*, 2015, no. 19–25 April 2015, pp. 1–11.
- [25] M. J. Moran and H. N. Shapiro, *Fundamentals of Engineering Thermodynamics*, 5th ed. England (UK): John Wiley & Sons, Inc., 2006.
- [26] Y. A. Cengel and M. A. Boles, *Thermodynamics: An Engineering Approach*, 8th ed. New York (US): Mc Graw Hill Education, 2015.
- [27] N. A. Pambudi, R. Itoi, S. Jalilinasrabady, and K. Jaelani, “Exergy analysis and optimization of Dieng single-Flash geothermal power plant,” *Energy Conversion and Management*, vol. 78, pp. 405–411, 2014.
- [28] M. Taghaddosi, “Conceptual Modelling of a Power Plant for the Sabalan Geothermal Area , Iran,” *UNU Geothermal Training Programme*, vol. Reports 20, no. 20, pp. 489–504, 2003.
- [29] N. A. Pambudi, R. Itoi, S. Jalilinasrabady, P. Sirait, and K. Jaelani, “Preliminary analysis of single flash combined with binary system using thermodynamic assessment: a case study of Dieng geothermal power plant,” *International Journal of Sustainable Engineering*, vol. 7038, no. October 2015, pp. 1–10, 2014.
- [30] C. R. Chamorro, M. E. Mondéjar, R. Ramos, J. J. Segovia, M. C. Martín, and M. A. Villamañán, “World geothermal power production status: Energy, environmental and economic study of high enthalpy technologies,” *Energy*, vol. 42, no. 1, pp. 10–18, 2012.
- [31] L. Bruscoli, D. Fiaschi, G. Manfrida, and D. Tempesti, “Improving the environmental sustainability of flash geothermal power plants-A case study,” *Sustainability (Switzerland)*, vol. 7, no. 11, pp. 15262–15283, 2015.
- [32] C. B. Kwambai, “Exergy Analysis of Olkaria I Power Plant , Kenya,” *UNU Geothermal Training Programme*, vol. Reports 5., no. 5, pp. 1–37, 2005.
- [33] R. E. D. Balqis, K. Indriawati, and B. L. W, “Optimasi Daya Listrik pada PT Pertamina Geothermal Energy Area Kamojang , Jawa Barat,” *Journal Teknik Pomits*, vol. 1, no. 1, pp. 1–6, 2012.
- [34] M. a. Rosen and R. Tang, “Improving steam power plant efficiency through exergy analysis: effects of altering excess combustion air and stack-gas temperature,” *International Journal of Exergy*, vol. 5, no. 1, pp. 31–51, 2008.
- [35] R. Adiprana, D. S. Purnomo, and I. E. Lubis, “Kamojang Geothermal Power Plant Unit 1-2-3 Evaluation and Optimization Based on Exergy Analysis,” in *Proceedings World Geothermal Congress, 19-25 April 2015*, 2015, no. April, pp. 19–25.
- [36] S. Jalilinasrabady, R. Itoi, P. Valdimarsson, G. Saevardottir, and H. Fujii, “Flash cycle optimization of Sabalan geothermal power plant employing exergy concept,” *Geothermics*, vol. 43, pp. 75–82, 2012.
- [37] M. Unverdi and Y. Cerci, “Performance analysis of Germencik Geothermal Power Plant,” *Energy*, vol. 52, pp. 192–200, 2013.
- [38] Y. Cerci, “Performance evaluation of a single-flash geothermal power plant in Denizli, Turkey,” *Energy*, vol. 28, no. 1, pp. 27–35, 2003.
- [39] M. R. Gomez, J. R. Gomez, L. M. Lopez-Gonzalez, and L. M. Lopez-Ochoa, “Thermodynamic analysis of a novel power plant with LNG (liquefied natural gas) cold exergy exploitation and CO2 capture,” *Energy*, vol. 105, pp. 32–44, 2016.
- [40] O.T. Winarno, Y. Alwandra, S. Mugiyanto, " Policies and Strategies for Renewable Energy Development in Indonesia", in 5th International Conference on Renewable Energy Research and Applications, 20-23 No 2016, ICRERA, Birmingham, UK, pp.270-272, 2016.
- [41] H. Ganjehsarabi, M. Asker, A.K. Seyhan, “Energy and exergy analyses of a solar assisted combined power and cooling cycle”, in 5th International Conference on Renewable Energy Research and Applications, 20-23 No 2016, ICRERA, Birmingham, UK, pp. 1141-1145,

2016.

[42] O. Özkaraca, P. Keçebas, C. Demircan, and A. Keçebas, “Thermodynamic Optimization of a GeothermalBased Organic Rankine Cycle System Using an Artificial Bee Colony Algorithm”, *Energies*, 10, 1691, pp. 1-27, 2017.

[43] Y. Ulusoy, A. H. Ulukardesler, R. Arslan, Y. Tekin, “Energy and emission benefits of chicken manure biogas production - A case study”, in 2017 IEEE 6th International Conference on Renewable Energy Research and Applications (ICRERA), pp. 648-652, 2017.

[44] C. Lazaroiu, M. Roscia, “Sustainable port through sea wave energy converter”, in 2017 IEEE 6th International Conference on Renewable Energy Research and Applications (ICRERA), pp. 462 – 467, 2017.

[45] B. Onat, Ü. A. Şahin, İ. Kırçova, G. Altınay, “Determination the relation between the target regulations about End of Life Vehicles (ELVs) and greenhouse gas emissions in Turkey”, in 2015 International Conference on Renewable Energy Research and Applications (ICRERA), pp.139 – 142, 2015.

Nomenclature

e specific exergy, (kJ/kg)

\dot{E} energy flow rate, (kW)
 h specific enthalpy, (kJ/kg)
 \dot{I}_{irr} irreversibility, (kW)
 \dot{m} mass flow rate, (kg/s)
 P pressure, (bar)
 s specific entropy, (kJ/kg-K)
 T temperature, (°C)
 \dot{W}_{gen} generator power, (kW)
 \dot{W}_{net} net power output, (kW)
 \dot{W}_{tur} turbine power, (kW)
 \dot{X}_{in} exergy inlet, (kW)
 \dot{X}_{br} exergy brine, (kW)
 \dot{X}_{tr} exergy transfer, (kW)
 \dot{X}_w exergy waste, (kW)

Greek letters

η_I energy efficiency, (%)
 η_{II} exergy efficiency, (%)
 η_{plant} power plant efficiency, (%)

Subscripts

i denotes the node i
 O denotes the dead state (reference state)
 I efficiency of the first law of thermodynamics
 II efficiency of the second law of thermodynamics
 tur turbin
 gen generator